Vol. 16, No. 2 (2017) 521-529

Catálisis, cinética y reactores

Revista Mexicana de Ingeniería Química

ULTRASONIC, ULTRAVIOLET, AND HYBRID CATALYTIC PROCESSES FOR THE DEGRADATION OF RHODAMINE B DYE: DECOLORIZATION KINETICS

PROCESOS CON RADIACIÓN ULTRASÓNICA, ULTRAVIOLETA Y CATALÍTICOS HÍBRIDOS DURANTE LA DEGRADACIÓN DEL COLORANTE RODAMINA B: CINÉTICA DE DECOLORACIÓN

J.A. Ayala, C.O. Castillo, R.S. Ruiz*

Grupo de Procesos de Transporte y Reacción en Sistemas Multifásicos, Depto. de IPH, Universidad Autónoma Metropolitana - Iztapalapa, Av. San Rafael Atlixco No. 186, C.P. 09340, México D.F., Mexico.

Received November 30, 2016; Accepted February 3, 2017

Abstract

The degradation of Rhodamine B dye was evaluated under different radiation conditions: sonolysis, photolysis, sonocatalysis, photocatalysis, and sonophotocatalysis, where commercial TiO_2 was utilized as catalyst. Color removal was monitored by spectrophotometry and mineralization was determined by TOC analysis. A two-first-order in-series reactions model was developed; it takes into consideration reaction times where the intermediates prevail. In this reaction scheme, the first reaction is the degradation of the coloured dye into coloured intermediates, and the second reaction is the conversion to colorless products. Good agreement was observed between experimental data and the developed kinetic model. The results suggest that dye degradation rate is more than one order of magnitude larger than the corresponding one for coloured degradation of intermediates. Under experimental conditions considered, water-soluble materials predominated over mineralized products within colorless products.

Keywords: synthetic dye, sonocatalysis, photocatalysis, hybrid process, kinetics.

Resumen

La degradación de la Rodamina B se evaluó bajo diferentes condiciones de radiación: sonólisis, fotólisis, sonocatálisis, fotocatálisis y un proceso híbrido de sonocatálisis y fotocatálisis, donde se utilizó TiO_2 comercial como catalizador. El seguimiento de las reacciones de degradación y mineralización de Rodamina B se llevó a cabo mediante espectrofotometría y análisis de carbón orgánico total (TOC), respectivamente. Se desarrolló un modelo cinético que considera un esquema de reacción en serie. El proceso hibrido presentó la mayor tasa de degradación y mineralización. En este esquema de reacción en serie, la primera reacción es la degradación del colorante a intermediarios orgánicos con color, y la segunda reacción es la degradación de estos intermediarios a compuestos sin color. El modelo ajustó adecuadamente las observaciones cinéticas. Los resultados sugieren que la velocidad de degradación de compuestos con color es mayor que la velocidad de degradación de compuestos sin color. A las condiciones de estudio evaluadas en este trabajo, la concentración de productos formados por el mecanismo de degradación de rodamina B a productos solubles en agua, fue mayor que la concentración de productos formados por el mecanismo de mineralización, óxidos de carbono, sales y agua.

Palabras clave: colorante sintético, sonocatálisis, fotocatálisis, proceso híbrido, cinética.

1 Introduction

Textile industry is in general one of the most water polluting industries, and it is estimated that around 10 to 20% of dyes are lost in the dyeing section of the industry due to process inefficiencies. Dyestuff in effluents disposed to water bodies imparts color and toxicity that are undesirable and harmful to the environment because of their refractory and carcinogenic nature (Barka *et al*., 2011). The presence of one or several benzene rings in the dye structure makes them highly stable molecules that are difficult to degrade by conventional chemical and biological methods (Pang *et al*., 2010). Therefore, several

* *Corresponding author. E-mail*: rmr@xanum.uam.mx

methods based on advanced oxidation processes such as photolysis, sonolysis and electrochemistry, have been developed for the removal of these pollutants from effluents by using hydroxyl radicals to degrade and mineralize the organic compounds (Aguilar *et al*., 2014; Barka *et al*., 2011; Pang *et al*., 2010; Priya *et al*., 2006; Tezcanli-Guyer and Ince, 2004).

Photocatalytic treatment has been considered as an attractive alternative for water treatment and mineralizing organic compounds to carbon dioxide, water and mineral acids (Pantoja-Espinoza *et al*., 2015; Moctezuma *et al*., 2016). In particular, the easy synthesis of TiO_2 and its semiconducting properties leading to high photoactivity make this material one of the most used to mineralize recalcitrant organic molecules (Ding *et al*., 1999; Saggioro, *et al*., 2011). However, some recent studies suggest the convenience of using combined or sequential methods over a single technique, i.e. process intensification. For instance, the combined operation of photocatalysis with sonolysis seems to enhance the photocatalytic efficiency and a synergetic effect between both technologies (Ertugay and Acar, 2016; Wu *et al*., 2014; Mathivanan *et al*., 2016). Both of these techniques, photocatalysis and sonolysis, have the potential of degrading dye molecules via $^{\cdot}OH$ attack. If the two radiation modes (UV and ultrasound) are operated in combination, a greater number of free radicals will be available for the reaction thereby increasing the rate of reactions. Equations (1) to (7) are typical of photocatalysis and Equation (9) denotes the contribution of ultrasound to radical formation, which can be extrapolated to sonocatalysis. In the case of sonolysis, ultrasound induces electrohydraulic cavitation in water and by which generated gas bubbles can implode violently generating local extreme conditions (5000 K and 1000 atm) under which water molecules readily disassociate as described by Eq. (9) (Priya and Madras, 2006). Furthermore, other possible reasons for the synergic effect between photocatalysis and sonocatalysis can be expected to include dispersion of aggregates of catalyst particles, refreshing of the TiO_2 surface, enhancement of mass transport, and pyrolysis in cavitation bubbles produced by ultrasound (Mathivanan *et al*., 2016).

$$TiO_2 + hv \rightarrow TiO_2(e^-) + TiO_2(h^+) \quad (1)$$

$$H_2O \rightarrow OH^-_{ads} + H^+ \quad (2)$$

$$h^+ + OH^-_{ads} \rightarrow {}^{\cdot}OH \quad (3)$$

$$e^- + O_2 \rightarrow O_2^{\cdot -} \quad (4)$$

$$H^+ + O_2 \rightarrow HO_2^{\cdot} \quad (5)$$

$$H^+ + O_2^{\cdot -} + HO_2^{\cdot} \rightarrow H_2O_2 + O_2 \quad (6)$$

$$H_2O_2 + hv \rightarrow 2\,{}^{\cdot}OH \quad (7)$$

$${}^{\cdot}OH + {}^{\cdot}OH \rightarrow H_2O_2 \quad (8)$$

$$H_2O+))) \rightarrow {}^{\cdot}OH + {}^{\cdot}H \quad (9)$$

Dye degradation and mineralization by $^{\cdot}OH$ attack is a gradual process that involves a series of reactions that generate several intermediate products. For instance, in studies on the photocatalytic degradation of Rhodamine B up to 25 different intermediate color and colorless products have been reported in the mineralization process (He *et al*., 2009; Natarajan *et al*., 2009). In this sense, understanding the kinetics of dye degradation under ultrasound and/or ultraviolet radiation processes seems essential to achieve higher efficiencies. In this regard, kinetic studies have been reported for diverse photocatalytic and sonocatalytic systems (e.g. Barka *et al*., 2011; Ding *et al*., 1999; Pang *et al*., 2010; Priya *et al*., 2006; Moctezuma *et al*., 2016; Tezcanli-Guyer and Ince, 2004; Saggioro, *et al*., 2011). For these systems literature studies have often presented their results in terms of first-order or Langmuir-Hinshelwood (L-H) kinetic models. This approach, however, focuses mainly on the degradation of a dye molecule. On this regard, kinetic analysis accounting for sequential reaction steps appears to be comparatively scarce and, to the best of our knowledge, it has not been reported previously for describing the hybrid process between photocatalysis and ultrasonically assisted catalysis, hereafter called sonophotocatalysis.

In the present work a model molecule, Rhodamine B basic dye, was degraded under different radiation conditions based on ultrasound and ultraviolet light and their combination. Ultrasonic, sonocatalytic, and sonophotocatalytic reaction results are then interpreted in terms of a two first-order in series reaction model that contemplates initial dye degradation into intermediate dyes and the further degradation of the latter into colorless material, which include both water-soluble molecules and mineralized products. The effect of the different operating conditions considered on reactor performance was discussed in terms of the variations observed in the relative magnitudes between the kinetic constants for dye and intermediate decomposition reactions, respectively.

2 Procedures

Rhodamine B purchased from J.T. Baker (99.8% purity) and distilled water were used in all the cases to prepare the desired concentration of the dye in the solution. Titanium dioxide (Degussa P-25) was used, when required, as catalyst. It had an average particle size of 30 nm and specific surface area of 55 m^2/g. The anatase and rutile percentage was 80 and 20% respectively.

Experiments were conducted in a 2.7 L thermostatic cylindrical Pyrex vessel, open to air, containing 1.0 L of the solution. In each experiment 30 mg L^{-1} RhB solution containing a previously determined optimum concentration of titanium dioxide (1.0 g L^{-1}) was sparged with air at a flow rate of 2.4 L min^{-1} (Alvarado-Camacho *et al*., 2014). An ultrasonic direct-immersion horn sonicator (Cole-Palmer TM), 20 kHz, 500 W, fitted with a 25 mm diameter probe, was utilized for generating ultrasonic sound waves in the reactor. The reaction vessel was also equipped with two 6 W ultraviolet lamps (with a maximum peak of 350 nm, 0.20 m long with 0.013 m diameter) which were immersed in axial position inside the reactor opposite two each other. The set-up used herein is shown in Fig. 1. To control the reactor temperature at the selected value of 25ºC (± 2 ºC) cold water from a thermostatic bath was pumped through the reactor jacket. The reactor was operated either under sonication, UV radiation, or under the combination of both modes of energy radiation. Samples were withdrawn from the reactor and centrifuged immediately for separation of the suspended solids with a centrifuge CHE SCIENTIFIC I, HKSC-220. All experiments were performed in triplicate and the average values are reported.

The remaining amount of Rhodamine B at a given time was determined by UV-vis spectroscopy. Every solution sample was analyzed for its absorbance at 554 nm using a HACH DR 6000^{TM} UV VIS Spectrophotometer with RFID Technology. The absorption was converted to a concentration through a calibration curve obtained using known concentration solutions of RhB using the Beer-Lambert law. Furthermore, mineralization of Rhodamine B solution was quantified from the decrease of total organic carbon. TOC was determined with a HACH DR200 Spectrophotometer, by means of HACH direct method 10129 for low range concentrations (0-20 mgL^{-1}). In this method total organic carbon standard solutions at known concentrations were used to obtain a calibration curve. Analysis of degradation and mineralization were performed in triplicate.

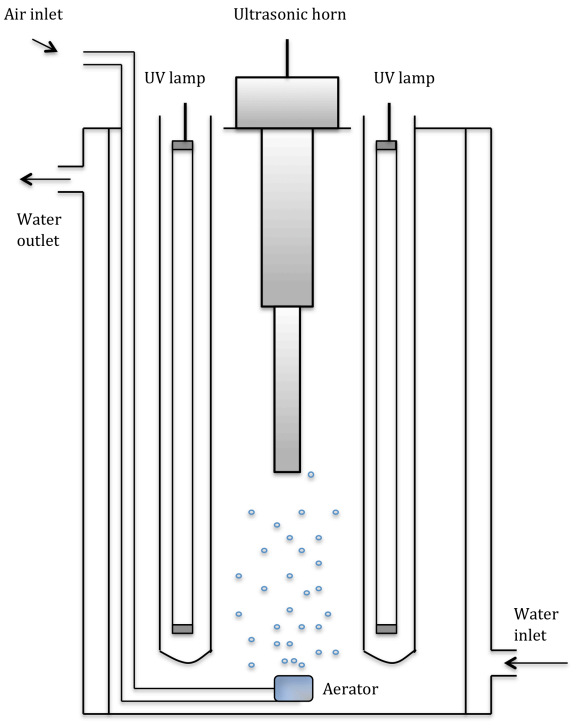

Fig. 1. Schematic diagram of experimental set-up.

3 Results and discussion

3.1 Ultraviolet (UV) degradation

Rhodamine B degradation profiles under ultraviolet conditions are shown in Fig. 2 for the following cases: i) in the absence of catalyst; ii) in the presence of catalyst; and iii) in the presence of both catalyst and ultrasonic radiation. As expected the photolysis alone appears to be the lowest efficient method of degradation among the three cases considered. In this regard, although dye degradation was favored by the presence of TiO_2 catalyst under photocatalytic conditions, larger degradation rates appear to occur under photosonocatalytic conditions. Although relatively small, the UV light had evident contribution on the dye degradation as also observed by other researchers (Natarajan *et al*., 2011; Tseng *et al*., 2011). The difference between direct photolysis and photocatalysis suggests that UV and TiO_2 photocatalyst have a synergic effect on the degradation of RhB. Since $^{\cdot}OH$ radicals are considered to be the dominant oxidizing species contributing to the photocatalytic degradation of organic substrates,

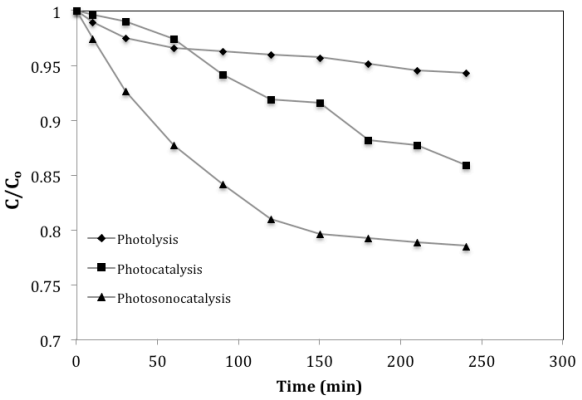

Fig. 2. Decolourization profiles of RhB solution under UV light radiation in the absence of catalyst, in presence of catalyst, and in presence of catalyst and in combination with ultrasound.

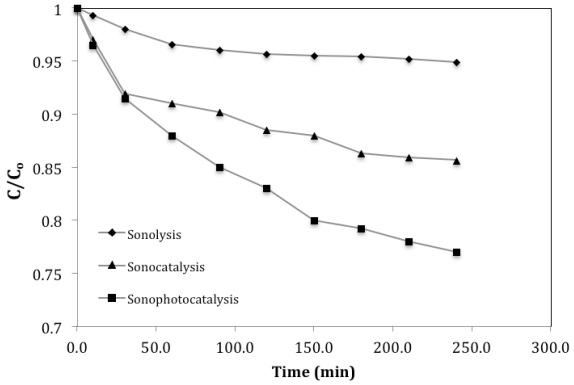

Fig. 3. Decolourization profiles of RhB solution under ultrasound in absence of catalyst, in presence of catalyst, and in the presence of catalyst in combination with UV light radiation.

dye degradation can be primarily associated to the generated ·OH radicals. Also shown in Fig. 2 is the degradation of rhodamine B for the case in which the catalytic system was simultaneously exposed to UV light and ultrasonic (US) radiation. It is clear that larger dye degradation rates were obtained for the UV/US/TiO_2 system in comparison with the UV treatments. The reason for this is that the basic mechanism for both ultrasonic and photocatalytic oxidations is the generation of free radicals. It is known that ultrasound waves with frequencies greater than 16 kHz can produce acoustic cavitation in water. The heat generated locally from the cavity implosion decomposes water and then highly reactive species are formed such as hydroxyl (·OH), hydrogen (·H), hydroperoxyl (·HO_2) radicals and hydrogen peroxide, which can readily react and degrade organic compounds (Joseph *et al*., 2009). Therefore, if these modes of radiation (UV and US) are operated in combination, an increase of the rate of reaction can result mainly from a larger number of radicals available for the reaction, nevertheless, a synergetic effect can also occur as ultrasound has been reported to enhance mass transport, catalyst particles dispersion, and refreshing of the TiO_2 surface.

3.2 Kinetics

Many researchers have reported that sonochemical degradation can be fitted to pseudo-first order kinetics (Behnajady *et al*., 2008; Inoue *et al*., 2006; Okitsu *et al*., 2005; Wang *et al*., 2003) or to Langmuir-Hinshelwood (L-H) type of models (Chiha *et al*, 2010; Merouani *et al*., 2010; Okitsu *et al*., 2005). Likewise, it has also been suggested pseudo-first order kinetics for sonocatalytic and photocatalytic degradation of dyes (Goel *et al*., 2004; Vinu and Madras, 2009; Pang *et al*., 2010b; Kavitha and Palanisamy, 2011; Joseph *et al*., 2012) or to L-H kinetic-type of models (Barka *et al*., 2011; Priya and Giridhar, 2006; Wu *et al*., 2014). In most of the reports discussing the first-order reaction kinetics, a simple semi logarithmic plot of log[C] (or ln[C], ln[C]/[C0], etc.) vs. time has been often used, and the information obtained is roughly analyzed to obey a pseudo-first order kinetic model (Okitsu *et al*., 2005). In the case of the studies that employ L-H type models have been limited to describe initial concentration changes. It can be expected, however, that reaction conditions change with time because products formed can scavenge generated ·OH radicals, and, hence, reported models may not be valid in longer reaction times where the effect of intermediate products prevail (Ghows and Entezari, 2013). Therefore, in the present work a kinetic approach that not only considers reaction of the original component, but also that of the intermediate products has been utilized, as depicted by Eq. (10), and in which the system is modeled by two first-order in-series reactions as suggested by other researchers (Ghows and Entezari, 2013; Julson and Ollis, 2006; Bergamini *et al*., 2009).

$$dyes \xrightarrow{k_1} intermediates \xrightarrow{k_2} colorless\ products \quad (10)$$

The sonolityc color removal data is presented in Fig. 4a in a semi log plot. It appears from this plot that a single straight line does not fit the data for the entire period of radiation, and instead two regions (dashed lines) can be identified that suggest a two first-order in-series reactions. Under these circumstances, assuming

that both reactions are first-order, eqs. (11) and (12) can describe the change of the concentrations with time of the dye and intermediates, respectively C_D and C_I, with the following initial conditions: for $t = 0$, $C_D = C_{D0}$ and $C_I = 0$.

$$\frac{dC_D}{dt} = -k_1 C_D \quad \Rightarrow C_D = C_{D0} e^{-k_1 t} \tag{11}$$

$$\frac{dC_I}{dt} = k_1 C_D - k_2 C_I \quad \Rightarrow C_I = \left(\frac{k_1 C_{D0}}{k_2 - k_1}\right)\left(e^{-k_1 t} - e^{-k_2 t}\right) \tag{12}$$

Measured absorbance is considered to be the sum of contributions from the dye and intermediates. Therefore, eq. (13) was obtained by combining Lambert-Beer equation ($Abs = \alpha_D C_D + \alpha_I C_I$) and eqs. (11) and (12), and where α_D and α_I are respectively the molar absorptivity of the dye and intermediates.

$$Abs_t = Abs_0 \left[\left(\frac{\alpha_I}{\alpha_D}\frac{k_1}{k_2 - k_1}\right)\left(e^{-k_1 t} - e^{-k_2 t}\right) + e^{-k_1 t}\right] \tag{13}$$

A nonlinear least-square algorithm (Levenberg-Marquardt) was applied to the experimental absorbance data to fit eq. (13) and from which the kinetic parameters k_1, k_2, and the ratio α_I/α_D were determined. The algorithm requires initial estimated values of these parameters for iteration purposes and they where obtained from the limiting cases of eq. (4) for both short and log times. For relatively long operating times, and by assuming that $k_1 \gg k_2$, Eq. (13) can be expressed as:

$$\ln\left(\frac{Abs_t}{Abs_0}\right) = \ln\left(\frac{\alpha_I}{\alpha_D k_2}\right) - k_2 t \tag{14}$$

The data in Figure 4a for sonication times larger than 50 min were fitted to Equation (14) by least squares and from which the required initial estimates for k_2 and α_I/α_D were obtained. At short times the exponential terms in Equation (14) were assumed to be described by the first two terms of the series expansion ($e^{-ax} \approx 1 - ax$) and after rearrangement yields Equation (15), which permits the calculation of a first estimate of the value of k_1.

$$k_1 = \frac{1 - \alpha_I/(k_2\alpha_D) - Abs_t/Abs_0}{t(1 + \alpha_I/(k_2\alpha_D))} \tag{15}$$

The obtained values for k_1 and k_2 with their respective 95 percent confidence limits, and the coefficient of determination R^2 are presented in Table 1.

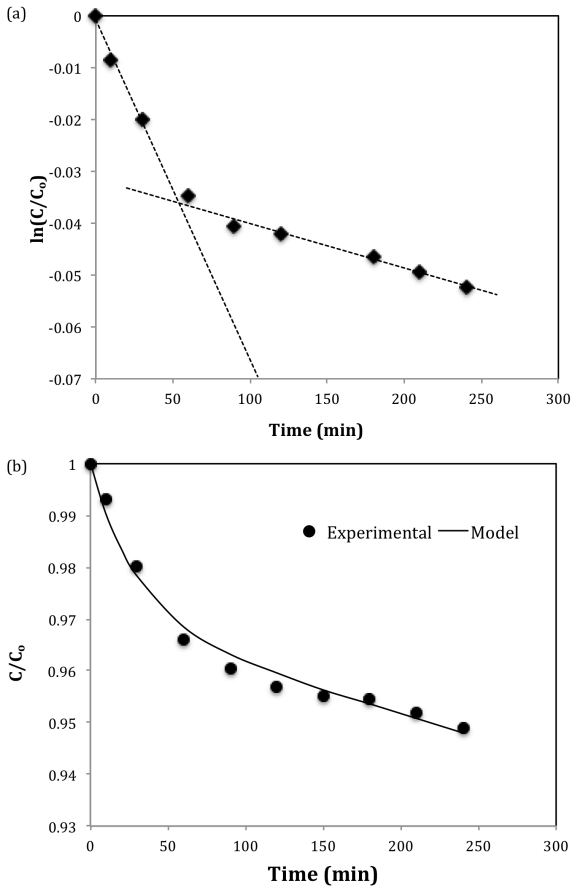

Fig. 4. Sonolytic color removal kinetic modelling: (a) plot suggesting a two-first order in-series reaction model and (b) model fitted to the experimental data.

Figure 4b shows both sonolytic experimental data and model predictions according to eq. (13), and from which it appears that the scheme accounting for the two first-order in-series reactions can satisfactorily fit the experimental data. It is evident from Table 1 that the reaction rate constant for original dye degradation is much larger than the corresponding one for the intermediates degradation ($k_1/k_2 = 319$). As was observed above for sonolysis degradation (Fig. 4a), two regions were also identified for both the degradation data for the sonolysis system in the presence of Titania particles as well as for the sonophotocatalytic system (see Figs. 5a and c). Therefore, the proposed scheme was assumed in each case and the respective data fitted to eq. (13). The obtained kinetic constants are presented in Table 1 and the experimental data model predictions are shown in Figs. 5b and d.

Table 1. Kinetic constants for ultrasound in the absence of catalyst, in the presence of catalyst, and in the presence of catalyst in combination with UV light radiation.

System	k_1 (min^{-1})	k_2 (min^{-1})	k_1/k_2	R^2
Sonolysis	$3.100\times10^{-2}\pm 0.620\times10^{-2}$	$9.717\times10^{-5}\pm 0.916\times10^{-5}$	319	0.999996
Sonocatalysis	$5.343\times10^{-2}\pm 1.631\times10^{-2}$	$3.135\times10^{-4}\pm 0.309\times10^{-4}$	170	0.999896
Sonophotocatalysis	$5.968\times10^{-2}\pm 3.853\times10^{-2}$	$8.760\times10^{-4}\pm 0.609\times10^{-4}$	68	0.999891

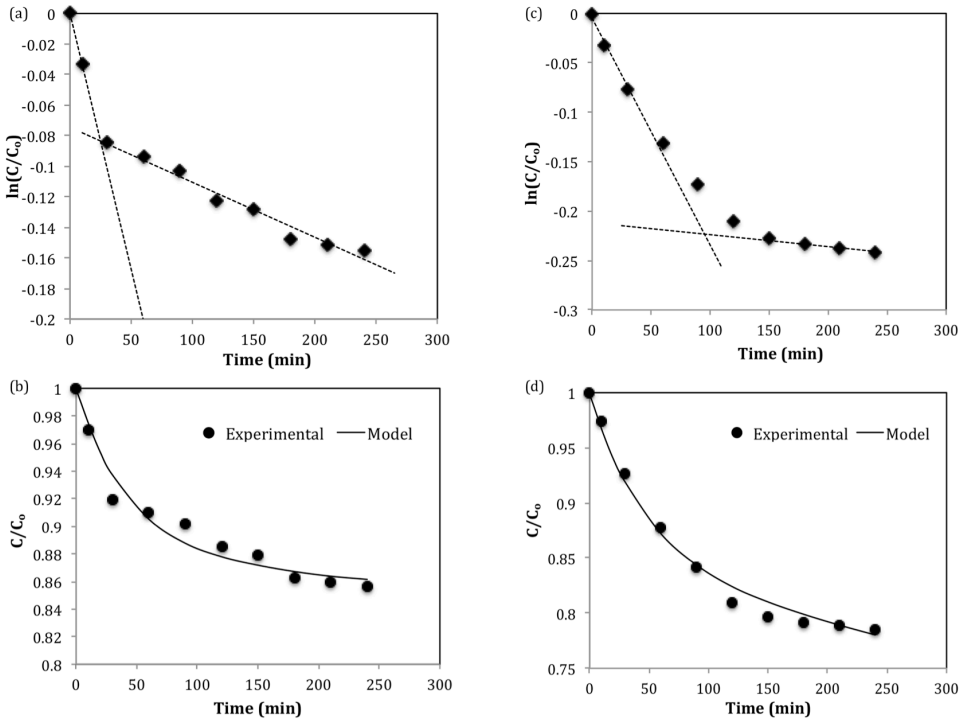

Fig. 5. Plot suggesting a two-first order in-series reaction model (a, c), and model fitted to the experimental data (b, d) for sonocatalytic and sonophotocatalytic colour removal kinetic modelling, respectively.

It is clear from Figure 5 that the proposed model is not only able to adequately represent the degradation data of Rhodamine B by sonocatalysis but also the corresponding degradation data by sonophotocatalysis. In both of these cases k_1 was found to be much larger than k_2, however when considering the three systems presented in Table 1 the relative importance between both reaction rates in terms of the ratio k_1/k_2 was found to be largest for sonolysis, somewhat lower for sonocatalysis, and the smallest for sonophotocatalysis. Albeit the apparent variations in k_1/k_2, the k_1 values reported in Table 1 for the three systems considered appear not to be statistically different between each other (95% confidence limit). For the case of k_2, however, significant differences were observed among the three operating modes considered, and it was the sonophotocatalytic system which showed the relatively largest k_2 value. This means that the intermediates are degraded faster using the three methods and the degradation of the dye is carried out with the same speed, independently of the method. In comparison with sonolytic degradation, the additional presence of titania particles (sonocatalysis) and, more significantly the combined operation of ultrasound with titania catalyst and UV radiation (sonophotocatalysis), not only can increase the total color degradation but also seem to promote the degradation rates of the intermediate products.

3.3 Color degradation and mineralization

Dye degradation produces color and colorless products, as well as mineralized material. The

extent of colorless and mineralized products as a function of degradation time was determined for sonophotocatalytic operation by measuring the Total Organic Carbon (TOC) during the process. Three lumps were assumed for the analysis: one expressed as dyes, which comprises color materials (C_{LD}); a second lump that includes all intermediate colorless products, (C_{LI}); and a third lump for mineralization products (C_{LM}). Lump concentrations were expressed in terms of carbon concentrations, and were calculated as follows:

$$C_{LM} = C_{LDo} - C_{TOC} \tag{16}$$

$$C_{LI} = C_{TOC} - C_{LD} \tag{17}$$

where C_{LDo} stands for the initial dyes carbon concentration and C_{TOC} refers to the measured TOC concentration at a given reaction time. C_{LD} is obtained from C_{Dye} (mgDye L^{-1}), determined by spectrophotometry, converted into carbon concentration by eq. (18), where m_C and m_{Dye} stand respectively for the weight of carbon in the dye molecule and for the dye molar weight.

$$C_{LD} = \frac{m_C}{m_{Dye}} C_{Dye} \tag{18}$$

Figure 6 presents the calculated dimensionless concentrations for intermediate colorless and mineralized product as calculated from eqs. (16) and (17) for sonophotocatalytic degradation of RhB (C_{Lj}/C_{LDo}). It appears that dyes degrade mainly into colorless products and that mineralized product such as CO_2 represent a comparatively smaller proportion for most of the experiment. It is also apparent in Fig. 6 that the concentration of colorless compounds reaches a maximum concentration after approximately 3 h of reaction, and that it tends to decline afterwards. Mineralized products concentration on the other hand augments slightly but continuously and seems to benefit from the increase of intermediate products degradation mentioned above. From these results it appears that intermediate color products are degraded mainly into colorless soluble products that are subsequently mineralized. Also shown in Fig. 6 is the total carbon concentration present in both colorless and mineralized products (C_{LI} + C_{LM}) and the corresponding calculated values based on the fitted model (eqs. (11)-(13)).

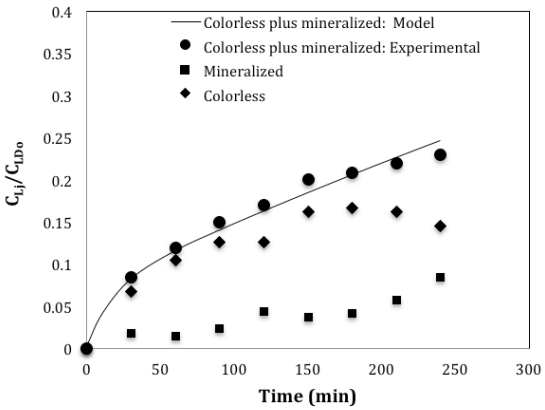

Fig. 6. Concentration profiles for colorless and mineralized intermediate products under sonophotocatalytic RhB dye degradation.

Conclusions

The degradation of Rhodamine B by solonolysis, sonocatalysis, photolysis, photocatalysis and sonophotocatalysis has been studied. It appears that degradation by sonolysis increases by the presence of TiO_2 particles and to further augment by sonophotocatalysis. Similarly, while photocatalysis improved photolysis degradation, sonophotocatalysis showed better performance. It appears for both sonolysis and photolysis that the presence of catalyst particles and the combined ultrasound-UV light operation can improve degradation rates by favoring the production of $^{\cdot}OH$ radicals, however, a synergetic effect from the dispersion of catalyst particle aggregates, cannot be discarded.

A two first-order in-series reactions model satisfactorily described color degradation under ultrasound, sonocatalysis, and sonophotocatalysis. In all three cases the dye degradation rate into color intermediates (k_1) was much faster than the degradation rate of the latter into colorless products (k_2). However, when compared with ultrasound operation, the magnitude of the kinetic constants for the degradation reactions of color intermediates appears to be the most favored by the presence of catalyst and by combined ultrasound-UV operation (k_2 showed a tenfold increase while k_1 doubled its magnitude). Regarding colorless products, they could be either as soluble or mineralized products. It was found that for the sonophotocatalysis process colorless products corresponded mainly to soluble products, which appeared to accumulate in solution and reach a maximum concentration before decreasing in favor of mineralized products.

References

Aguilar, O., Angeles, C., Castillo, C.O., Martínez, C., Rodríguez, R., Ruiz, R.S., and Vizcarra, M.G. (2014). On the ultrasonic degradation of Rhodamine B in water: kinetics and operational conditions effect. *Environmental Technology 35*, 1183-1189.

Alvarado Camacho, C., Couder García, M., Méndez Salazar, S., Emily Moreno Barreta, E., Ruiz Martínez, R.S., Castillo Araiza, C.O. (2014) Estudio cinético de la degradación fotocatalítica de Rodamina B utilizando catalizadores a base de TiO_2 (TiO_2 DP25, TiO_2-Zr y TiO_2-B), In *Memorias del XXXVI Encuentro Nacional de la AMIDIQ*, 3227-3230.

Barka, N., Qourzal, S., Assabbane, A., Nounah, A. and Ait-Ichou, Y. (2011). Photocatalytic degradation of patent blue V by supported TiO_2: kinetics, mineralization, and reaction pathway. *Chemical Engineering Communications 198*, 1233-1243.

Behnajady, M.A., Modirshahla, N., Tabrizi, S.B., and Molanee, S. (2008). Ultrasonic degradation of Rhodamine B in aqueous solution: Influence of operational parameters. *Journal of Hazardous Materials 152*, 381-386.

Bergamini, R.B.M., Azevedo, E.B., and Araújo, L.R.D. (2009). Heterogeneous photocatalytic degradation of reactive dyes in aqueous TiO_2 suspensions: Decolorization kinetics. *Chemical Engineering Journal 149*, 215-220.

Chen, Y.C., Vorontsov, A.V., and Smirniotis, P.G. (2003). Enhanced photocatalytic degradation of dimethyl methylphosphonate in the presence of low-frequency ultrasound. *Photochemical & Photobiological Sciences 2*, 694-698.

Chiha, M., Merouani, S., Hamdaoui, O., Baup, S., Gondrexon, N., and Pétrier C. (2010) Modeling of ultrasonic degradation of non-volatile organic compounds by Langmuir-type kinetics. *Ultrasonics Sonochemistry 17*, 773-782.

Ding, Z., Zhu, H.Y., Lu G.Q., and Greenfield, P.F. (1999). Photocatalytic properties of titania pillared clays by different drying methods. *Journal of Colloid and Interface Science 209*, 193-199.

Eren, Z., and Ince, N.H. (2010). Sonolytic and sonocatalytic degradation of azo dyes by low and high frequency ultrasound. *Journal of Hazardous Materials 177*, 1019-1024.

Ertugay, N., and Acar, F.N. (2016). Decolorization of Direct Blue 71 using UV irradiation and ultrasound in the presence of TiO_2 catalyst. *Desalination and Water Treatment 57*, 9318-9324.

Ghows, N., and Entezari, M.H. (2013). Kinetic investigation on sono-degradation of Reactive Black 5 with core-shell nanocrystal. *Ultrasonics Sonochemistry 20*, 386-394.

Goel, M., Hongqiang, H., Mujumdar, A.S., and Ray, M.B. (2004). Sonochemical decomposition of volatile and non-volatile organic compounds-a comparative study. *Water Research 38*, 4247-4261.

He, Z., Sun, C., Yang, S., Ding, Y., He, H., and Wang, Z. (2009). Photocatalytic degradation of rhodamine B by Bi_2WO_6 with electron accepting agent under microwave irradiation: mechanism and pathway. *Journal of Hazardous Materials 162*, 1477-1486.

Inoue, M., Okada, F., Sakurai, A., and Sakakibara, M. (2006). A new development of dyestuffs degradation system using ultrasound. *Ultrasonics Sonochemistry 13*, 313-320.

Joseph, C.G., Liew, Y.L.S., Krishnaiah, D., and Bono, A. (2012). Application of a semiconductor oxide-based catalyst in heterogeneous wastewater treatment: a green technology approach. *Journal of Applied Sciences 12*, 1966-1971.

Julson, A.J., and Ollis, D.F. (2006). Kinetics of dye decolorization in an air-solid system. *Applied Catalysis B: Environmental 65*, 315-325.

Kavitha, S.K., and Palanisamy, P.N. (2011). Photocatalytic and sonophotocatalytic degradation of Reactive Red 120 using dye sensitized TiO_2 under visible light. *International Journal of Chemical, Molecular, Nuclear, Materials and Metallurgical Engineering 5*, 1-6.

Mathivanan, V., Geetha Manjari. S., Ineya. R., Saravanathaamizhan, R., Senthil Kumar, P., and Ramakrishnan, K. (2016). Enhanced photocatalytic decolorizationof reactive red by sonocatalysis using TiO_2 catalyst: factorial design of experiments. *Desalination and Water Treatment 57*, 7120-7129.

Moctezuma, E., López-Barragán, M.A., and Zermeño-Resendiz, B.B. (2016) Rutas de reacción para la degradación fotocatalítica de soluciones de fenol bajo diferentes condiciones experimentales. *Revista Mexicana de Ingeniería Química 15*, 129-137.

Merouani, S., Hamdaoui, O., Saoudi, F., and Chiha, M. (2010). Sonochemical degradation of Rhodamine B in aqueous phase: Effects of additives. *Chemical Engineering Journal 158*, 550-557.

Natarajan, T.S., Thomas, M., Natarajan, K., Bajaj, H.C., and Tayade, J.T. (2011). Study on UV_LED/TiO_2 process for degradation of Rhodamine B dye. *Chemical Engineering Journal 169*, 126-134.

Okitsu, K., Iwasaki, K., Yobiko, Y., Bandow., H., Nishimura, R., and Maeda, Y. (2005). Sonochemical degradation of azo dyes in aqueous solution: a new heterogeneous kinetics model taking into account the local concentration of OH radicals and azo dyes. *Ultrasonics Sonochemistry 12*, 255-262.

Pang, Y.L., Abdullah, A.Z., and Bathia, S. (2010a). Comparison of sonocatalytic activities on the degradation of Rhodamine B in the presence of TiO_2 powder and nanotubes. *Journal of Applied Sciences 10*, 1068-1075.

Pang, Y.L., Abdullah, A.Z., and Bhatia, S. (2010b). Effect of annealing temperature on the characteristics, sonocatalytic activity and reusability of nanotubes TiO_2 in the degradation of Rhodamine B. *Applied Catalysis B Environmental 100*, 393-402.

Pantoja-Espinoza, J.C., Proal-Nájera, J.B., García-Roig, M., Chairez-Hernández, I., and Osorio-Revilla, G.I. (2015). Eficiencias comparativas de inactivación de bacterias coliforms en efluentes municipals por fotólisis (UV) y por fotocatálisis (UV/TiO_2/SiO_2). Caso: Depuradora de aguas de Salamanca, España. *Revista Mexicana de Ingeniería Química 14*, 119-135.

Priya, M.H., and Madras, G. (2006) Kinetics of TiO_2-catalyzed ultrasonic degradation of rhodamine dyes. *Industrial & Engineering Chemical Research 45*, 913-921.

Saggioro, E.M., Oliveira, A.S., Pavesi, T., Maia, C.G., Ferreira, L.F., and Moreira, J.C. (2011). Use of titanium dioxide photocatalysis on the remediation of model textile wastewaters containing azo dyes. *Molecules 16*, 10370-10386.

Shimizu, N., Ogino, C., Dadjour, M.F., and Murata, T. (2007). Sonocatalytic degradation of methylene blue with TiO_2 pellets in water. *Ultrasonics Sonochemistry 14*, 184-190.

Tezcanli-Guyer, G., and Ince, N.H. (2004) Individual and combined effects of ultrasound, ozone and UV irradiation: a case study with textile dyes. *Ultrasonics 42*, 603-609.

Tseng, D.H., Juang, L.C., and Huang, H.H. (2012). Effect of oxygen and hydrogen peroxide on the photocatalytic degradation of monochlorobenzene in TiO_2 aqueous suspension. *International Journal of Photoenergy 2012*, Article ID 328526, 9 pages doi:10.1155/2012/328526.

Vinu, R., and Madras, G. (2009). Kinetics of sonophotocatalytic degradation of anionic dyes with nano-TiO_2. *Environmental Science and Technology 43*, 473-479.

Wang, X.K., Chen, G.H., and Guo, W.L. (2003). Sonochemical degradation kinetics of methyl violet in aqueous solutions. *Molecules 8*, 40-44.

Wu, C.D., Zhang, J.Y., Wu, Y., and Wu, G.Z. (2014). Degradation of phenol in water by the combination of sonolysis and photocatalysis. *Desalination and Water Treatment 52*, 1911-1918.